# Role of impurities in determining the exciton diffusion length in organic semiconductors

Ian J. Curtin,[1] D. Wayne Blaylock,[2] Russell J. Holmes[1]

[1]Department of Chemical Engineering and Materials Science, University of Minnesota, Minneapolis, Minnesota 55455

[2]Engineering and Process Sciences, Core R&D, The Dow Chemical Company, Midland, Michigan, 48674, USA

## Abstract

The design and performance of organic photovoltaic cells is dictated in part by the magnitude of the exciton diffusion length ($L_D$). Despite the importance of this parameter, there have been few investigations connecting $L_D$ and materials purity. Here, we investigate $L_D$ for the organic small molecule *N*,*N*′-bis(naphthalen-1-yl)-*N*,*N*′-bis(phenyl)-benzidine (α-NPD) as native impurities are systematically removed from the material. Thin films deposited from the as-synthesized material yield an $L_D$, as measured by photoluminescence quenching, of (3.9 ± 0.5) nm with a corresponding photoluminescence efficiency ($\eta_{PL}$) of (25 ± 1)% and thin film purity of (97.1 ± 1.2)%, measured by high performance liquid chromatography. After purification by thermal gradient sublimation, the value of $L_D$ is increased to (4.7 ± 0.5) nm with a corresponding $\eta_{PL}$ of (33 ± 1)% and purity of (98.3 ± 0.8)%. Interestingly, a similar behavior is also observed as a function of the deposition boat temperature. Films grown from the purified material at a high temperature give $L_D$ = (5.3 ± 0.8) nm with $\eta_{PL}$= (37 ± 1)% for films with a purity of (99.0 ± 0.3)% purity. Using a model of diffusion by Förster energy transfer, the variation of $L_D$ with purity is predicted as a function of $\eta_{PL}$ and is in good agreement with measurements. The removal of impurities acts to decrease the non-radiative exciton decay rate and increase the

radiative decay rate, leading to increases in both the diffusivity and exciton lifetime. The results of this work highlight the role of impurities in determining $L_D$, while also providing insight into the degree of materials purification necessary to achieve optimized exciton transport.

The optical excitation of an organic semiconductor leads to the formation of tightly bound molecular excited states termed excitons.[1] Organic photovoltaic devices (OPVs) based on these materials rely on the use of an energetic electron donor-acceptor heterojunction to dissociate photogenerated excitons into a useable photocurrent. Device architecture is dictated in large part by the intrinsically short exciton diffusion length ($L_D$ ~ 10 nm),[2–8] which is the characteristic distance an exciton can travel before it recombines.[9] While a great deal of work has focused on optimizing the morphology of active layer blends in bulk heterojunction devices in order to circumvent the short $L_D$,[5,10–13] substantially less attention has been directed at investigating the origin of the near universally short $L_D$. As such, it remains important to understand the mechanisms which control and ultimately limit $L_D$ in order to better inform material and device design for longer $L_D$ and enhanced device efficiency. One aspect of exciton diffusion that remains relatively unexplored is how material purity affects $L_D$.[7,14] While previous work has shown how impurities affect carrier mobility and overall device performance, an analogous understanding for the role of impurities in exciton energy transfer and diffusion is lacking.[15–19] In this work, $L_D$ and other relevant photophysical parameters are measured as native molecular impurities are systematically removed from films of *N*,*N*′-bis(naphthalen-1-yl)-*N*,*N*′-bis(phenyl)-benzidine (α-NPD). By modelling the observed trend in $L_D$ as a function of impurity concentration, an impurity free, theoretical maximum value of $L_D$ for α-NPD is extracted.

Exciton diffusion in organic semiconductors occurs due to an ensemble of excitons undergoing successive energy transfer hops between molecules of the same species.[20] In fluorescent materials including α-NPD, the dominant mechanism of energy transfer is Förster transfer.[3,21,22] The rate of energy transfer for this process is given by,

$$k_F = \frac{1}{\tau}\left(\frac{R_0}{d}\right)^6 \quad (1)$$

where d is the intermolecular spacing and $R_o$ is the Förster radius, which is defined as the critical distance at which the rate of Förster transfer equals the rate of all other excitonic decay pathways.[21] The exciton lifetime ($\tau$) can be separately expressed in terms of the radiative ($k_R$) and non-radiative ($k_{NR}$) exciton recombination rates as $\tau = (k_R + k_{NR})^{-1}$.[23] Additionally, $R_o$ can be broken down further and written in terms of physically measureable quantities as:[21,23,24]

$$R_0{}^6 = \frac{9\eta_{PL}\kappa^2}{128\pi^5 n^4}\int \lambda^4 F_D(\lambda)\sigma_A(\lambda)d\lambda \quad (2)$$

where $F_D$ is the area normalized fluorescence spectrum, $\sigma_A$ is the absorption cross section, $\lambda$ is the wavelength of light, n is the refractive index at the wavelength where the overlap of the emission and absorption are maximized and $\kappa$ is the dipole orientation factor. Plots of $\sigma_A(\lambda)$ and $F_D(\lambda)$ for α-NPD are shown in Fig. 1; $\sigma_A$ is calculated as $4\pi k/\lambda\rho$ where k is the extinction coefficient, extracted from ellipsometric measurements, and $\rho$ is the molecular density.[25] The photoluminescence (PL) efficiency ($\eta_{PL}$) is given by ratio of $k_R$ to the total rate of exciton recombination and can be written as, $\eta_{PL} = k_R\tau$. The orientation factor, $\kappa$, describes the degree of electromagnetic coupling between the transition dipoles of the two molecules involved in the energy transfer event. For randomly oriented rigid dipoles found in amorphous materials such as α-NPD, $\kappa = 0.845\sqrt{2/3}$.[26]

Exciton diffusion is frequently modeled as a series of self-energy transfer hops on a simple cubic lattice.[3,20] By restricting energy transfer to the six nearest neighbors, a generalized diffusion coefficient can be written as $D = d^2k_{ET,}$ where d is the lattice constant and $k_{ET}$ is the energy transfer rate.[20,27] Taking $k_{ET}$ to be the rate of Förster transfer, $k_F$ from Eqn. 1, $L_D$ may be written using Eqn. 2 and $L_D = \sqrt{D\tau}$ as:

$$L_D = \frac{R_0{}^3}{d^2} = \frac{1}{d^2}\sqrt{\frac{9\eta_{PL}\kappa^2}{128\pi^5 n^4}\int \lambda^4 F_D(\lambda)\sigma_A(\lambda)d\lambda} \quad (3)$$

Although the role of impurities is not explicitly included in Eqn. 3, we hypothesize that molecular impurities which quench excitons will act to reduce $\tau$, $\eta_{PL}$ and ultimately $L_{D.}$

Photoluminescence quenching based measurements are among the most widely employed techniques to determine $L_D$. This type of measurement can be applied in either the transient regime[28] or the steady state regime, through spectrally resolved[3] or thickness dependent PL quenching[27], as shown in this work. In thickness dependent PL quenching, a series of α-NPD films are grown over a range of thicknesses, both with and without an adjacent quenching layer. An exciton quenching layer of dipyrazino[2,3-f:2',3'-h]quinoxaline-2,3,6,7,10,11-hexacarbonitrile (HATCN) is used due to its favorable energy offset for electron transfer and large energy gap which prevents Förster transfer from α-NPD to HATCN.[24] Under optical excitation, the PL is inversely proportional to the fraction of excitons which successfully diffuse to the donor/quencher interface. PL ratios are constructed by dividing the integrated PL spectrum of the quenched film by that of the unquenched film. $L_D$ is then extracted by modelling the PL ratio as a function of donor layer thickness using a one-dimensional steady-state exciton diffusion equation which explicitly calculates the generating optical field through the use of a transfer matrix formalism.[29] Experimentally obtained PL ratios as a function of α-NPD thin film thickness are shown in Fig. 2. The α-NPD source material was synthesized by The Dow Chemical Company. All samples were deposited on glass substrates by thermal vacuum sublimation at a base pressure of $7x10^{-7}$ Torr, with deposition pressures $\leq$ $9x10^{-7}$ Torr. Additionally, fresh source material was loaded for each deposition in order to assure a constant starting source material purity for all thicknesses considered. Thin film purities were measured using high performance liquid chromatography (HPLC). Concentrated samples were prepared by dissolving multiple 100-nm-thick films of α-NPD in tetrahydrofuran. Purities were determined

by HPLC area percent assay and are listed in Table 1. Additionally, a more detailed table of the HPLC results is shown in Table S1.[30] X-ray diffraction spectra were measured on 80-nm-thick α-NPD films deposited on silicon substrates using a Bruker Co Kα source x-ray diffractometer.

Films made from the as-synthesized source material yield $L_D$ = (3.9 ± 0.5) nm with a corresponding thin film organic purity of (97.1 ± 1.2)%. The source material was then purified once via vacuum thermal gradient sublimation.[31,32] Films deposited from the purified source material show an increased value of $L_D$ = (4.7 ± 0.5) nm and purity of (98.3 ± 0.8)%. Interestingly, it was also observed that the value of $L_D$ and thin film purity showed a dependence on the deposition boat temperature. Initial films were grown at a deposition boat temperature of (258 ± 10)$^o$C, corresponding to a deposition rate of 0.3 Å/s. As the boat temperature was increased to (324 ± 10)$^o$C with a deposition rate of 8.8 Å/s, films deposited from the purified source material showed an increase in $L_D$, reaching a value of $L_D$ = (5.3 ± 0.9) nm and purity of (99.0 ± 0.3)%. This represents at 36% increase in $L_D$ as the purity of the α-NPD films is increased by 1.9%.

In order to further probe the role of impurities in determining $L_D$, $\eta_{PL}$ and $\tau$ were measured for all samples and are listed in Table 1, additionally, lifetime decays are shown in Fig. S1.[30] It was observed that increases in $L_D$ and purity coincide with concomitant increases in both $\eta_{PL}$ and $\tau$. Films with a purity of 97.1% yield values of $\eta_{PL}$ = (25 ± 1)% and $\tau$ = (2.7 ± 0.1) ns. These values increase to $\eta_{PL}$ = (37 ± 1)% and $\tau$ = (3.3 ± 0.1) ns for the 99.0% pure films. Based on the observed increases in $\eta_{PL}$ and $\tau$, the corresponding values of $k_R$ and $k_{NR}$ can be extracted. For an increase in film purity from 97.1% to the 99.0%, $k_{NR}$ systematically decreases from (28 ± 2)×$10^7$ $s^{-1}$ to (19 ± 1)×$10^7$ $s^{-1}$, driving an increase in $\tau$, and offering the exciton more time to diffuse before undergoing recombination. For the same change in purity, $k_R$ increases from (9.3

$\pm 0.5)\times10^7\ s^{-1}$ to $(11 \pm 1)\times10^7\ s^{-1}$. Upon inspection of Eqns. 1 and 2 and given the relationship $D = d^2k_F$, it is clear that D is proportional to $k_R$. Thus, the increase in $k_R$ is also driving an increase in D, due to an enhanced Förster radius.

Based on the observed enhancement in the photophysics, predictions of $L_D$ can be made using a conventional model of diffusion by Förster transfer using Eqn. 3. A value of d = 0.58 nm was calculated from the volume averaged radius using the crystal density of α-NPD.[3,25] Values of the predicted $L_D$ are listed in Table 1 and are in good agreement with the experimentally measured values, confirming that changes in $\eta_{PL}$ and $\tau$ are responsible for the observed trend in $L_D$. Additionally, x-ray diffraction spectra taken on the films revealed no scattering peaks, ruling out crystallinity as a possible explanation of the change in the photophysics.[2,33,34] Given the correlation between the photophysics, $L_D$ and film purity, we conclude that the improvements in performance are caused by a reduction in the concentration of exciton quenching impurities present in the films. Furthermore, the dependence of $L_D$ on the deposition boat temperature comes from additional material purification during the deposition process.

If a molecular impurity provides an additional non-radiative decay channel to diffusing excitons, two of the most obvious mechanisms by which this deexcitation could occur are exciton dissociation by charge transfer and exciton quenching by Förster transfer. A charge transfer impurity would require a sufficient energy level offset necessary for electron or hole transfer and would occur on a nearest neighbor length scale.[23] Förster transfer impurities would require an overlap in the absorption spectrum of the impurity molecule and the fluorescence spectrum of α-NPD.[21,24] In this scenario, a diffusing exciton may transfer to an impurity molecule, where it would eventually decay non-radiatively. This interaction could occur over a

longer length scale consistent with Eqn. 1.[21] Thus, we expect Förster transfer impurities to be more detrimental than charge transfer impurities for a given impurity concentration.

The effect impurities have on $L_D$ can be modelled through the use of a simple one dimensional steady state diffusion equation:

$$0 = D\frac{\partial^2 n}{\partial x^2} - \frac{n}{\tau_o} + G - nk_Q \tag{4}$$

Here, n is the exciton density, D is the diffusion coefficient, $\tau_o$ is the natural lifetime in the absence of impurities, G is the optical exciton generation rate and $k_Q$ is the average rate of exciton quenching by impurities in the steady state. Previously, it was shown that impurities primarily affect $k_{NR}$. Thus, $k_{NR}$ can be expressed as the sum of the component losses, $k_{NR} = (k_{NR}^{o} + k_Q)$, where $k_{NR}^{o}$ is the intrinsic non-radiative decay rate and therefore $1/\tau = (k_R + k_{NR}^{o} + k_Q) = 1/\tau_o + k_Q$. Here, we consider the case of exciton quenching by Förster transfer to impurities. The transfer rate for an exciton on a single host molecule transferring to an impurity molecule is described by Eqn 1. It has been previously argued however that for an exciton interacting with a distribution of impurities, the quenching rate must be multiplied by the molecular density of the impurities and integrated over all of space.[35] This yields the following average quenching rate of excitons by impurities,

$$k_Q = \frac{R_I^6 Q}{d^6 \tau_o} \tag{5}$$

where Q is the fraction of impurity molecules and $R_I$ is the Förster radius from the host molecule to the impurity. Inserting Eqn. 5 into Eqn. 4 and solving yields a simple expression for the effective $L_D$ as a function of impurity concentration:

$$L_D = \sqrt{\frac{D\tau_0}{1+\frac{R_I^6 Q}{d^6}}} = \sqrt{\frac{L_{D,0}^2}{1+\frac{R_I^6 Q}{d^6}}}. \tag{6}$$

Here, $L_{D,0}$ represents the diffusion length in the absence of impurities. Using Eqn. 6, the experimental values of $L_D$ are well fit as a function of the impurity fraction determined from HPLC, as shown in Fig. 3. This yields a Förster radius of $R_I$ = (1.3 ± 0.1) nm and $L_{D,0}$ = (7.0 ± 1.0) nm. From Fig. 3, it can be seen that dramatic improvements in $L_D$ can be made as the film purity is increased beyond 99%, stressing the importance of attaining high materials purity in achieving a maximum $L_D$.

While this model fits the data well, it is not without its limitations. With multiple impurity species present in the films, the extracted value of $R_I$ represents an average Förster radius for all impurities within the film, when in actuality each separate impurity would have its own characteristic Förster radius. Furthermore, there is no way to distinguish between Förster and charge transfer impurities with the data set of Fig. 3. Following the procedure outlined in Eqns. 4-6 and instead inserting a charge transfer rate would produce the same dependence on Q and the same fit. In order to definitively distinguish the mechanism by which these impurities are reducing $L_D$, the native impurities would need to be chemically identified and synthesized in order to determine their absorption spectra and energy levels. These molecules could then be controllably doped back into ultra-pure films of α-NPD in order to attain a more accurate and quantitative understanding of which impurities are reducing $L_D$ and by what mechanism.

In summary, we have demonstrated that native molecular impurities present in organic semiconductors can impede exciton diffusion by measuring $L_D$ as native molecular impurities are systematically removed from films of α-NPD. In this work, $L_D$ was increased from (3.9 ± 0.5) nm to (5.3 ± 0.9) nm as the thin film HPLC purity increased from 97.1% to 99.0%. Increases in $L_D$ are caused by a reduction in the concentration of exciton quenching impurities, which acts to reduce $k_{NR}$ and increase $k_R$, $\tau$ and D. Experimentally measured values of $L_D$ agree with predicted

values calculated as a function of $\eta_{PL,}$ using a diffusion model based on Förster energy transfer. Furthermore, the trend of $L_D$ as a function of impurity concentration is well-fit using a model which assumes exciton quenching by Förster transfer. This work provides insight into role of molecular impurities in determining $L_D$ and a reference for what degree of material purification is necessary to achieve optimized exciton transport.

**Acknowledgments:**

This work was supported by the National Science Foundation (NSF) under DMR-1307066. IJC also acknowledges support from the Robert and Beverly Sundahl Fellowship. All materials synthesis and HPLC was performed at The Dow Chemical Company.

**References:**


[1] N. Turro, V. Ramamurthy, and J.C. Scaiano, *Principles of Modern Molecular Photochemsitry* (2009).

[2] R.R. Lunt, J.B. Benziger, and S.R. Forrest, Adv. Mater. **22**, 1233 (2010).

[3] R.R. Lunt, N.C. Giebink, A. A. Belak, J.B. Benziger, and S.R. Forrest, J. Appl. Phys. **105**, 053711 (2009).

[4] K.J. Bergemann, X. Liu, A. Panda, and S.R. Forrest, Phys. Rev. B **92**, 035408 (2015).

[5] G. Wei, R.R. Lunt, K. Sun, S. Wang, M.E. Thompson, and S.R. Forrest, Nano Lett. **10**, 3555 (2010).

[6] S. Hofmann, T.C. Rosenow, M.C. Gather, B. Lüssem, and K. Leo, Phys. Rev. B **85**, 245209 (2012).

[7] O. V. Mikhnenko, M. Kuik, J. Lin, N. van der Kaap, T.Q. Nguyen, and P.W.M. Blom, Adv. Mater. **26**, 1912 (2014).

[8] F. Piersimoni, D. Cheyns, K. Vandewal, J. V Manca, and B.P. Rand, J. Phys. Chem. Lett. **3**, 2064 (2012).

[9] P. Peumans, A. Yakimov, and S.R. Forrest, J. Appl. Phys. **93**, 3693 (2003).

[10] R. Pandey and R.J. Holmes, Adv. Mater. **22**, 5301 (2010).

[11] P. Peumans, S. Uchida, and S.R. Forrest, Nature **425**, 158 (2003).

[12] W.A. Luhman and R.J. Holmes, Appl. Phys. Lett. **94**, 153304 (2009).

[13] R.R. Lunt, J.B. Benziger, and S.R. Forrest, Adv. Mater. **22**, 1233 (2010).

[14] S. Athanasopoulos, E. Hennebicq, D. Beljonne, and A.B. Walker, Phys. Chem. C **112**, 11532 (2008).

[15] R. Salzman, J. Xue, B. Rand, A. Alexander, M. Thompson, and S. Forrest, Org. Electron. **6**, 242 (2005).

[16] J. Drechsel, A. Petrich, M. Koch, S. Pfützner, R. Meerheim, S. Scholz, K. Walzer, M. Pfeiffer, and K. Leo, Dig. Tech. Pap. **37**, 1962 (2006).

[17] S.Z. Bisri, T. Takenobu, T. Takahashi, and Y. Iwasa, Appl. Phys. Lett. **96**, 183304 (2010).

[18] L. Kaake, X.D. Dang, W.L. Leong, Y. Zhang, A. Heeger, and T.Q. Nguyen, Adv. Mater. **25**, 1706 (2013).

[19] M.P. Nikiforov, B. Lai, W. Chen, S. Chen, R.D. Schaller, J. Strzalka, J. Maser, and S.B. Darling, Energy Environ. Sci. **6**, 1513 (2013).

[20] R.C. Powell and Z.G. Soos, J. Lumin. **11**, 1 (1975).

[21] T. Forster, R. Soc. Chemsitry **27**, 7 (1959).

[22] S.M. Menke, W.A. Luhman, and R.J. Holmes, Nat. Mater. **12**, 152 (2013).

[23] M. Pope and C. Swenberg, *Electronic Processes in Organic Crystals*, 1st ed. (Oxford University Press, 1982).

[24] W.A. Luhman and R.J. Holmes, Adv. Funct. Mater. **21**, 764 (2011).

[25] J.A. Cheng and P.J. Cheng, J. Chem. Crystallogr. **40**, 557 (2010).

[26] M.Z. Maksimov and I.M. Rozman, Opt. Spectrosc. **12**, 337 (1962).

[27] S.M. Menke and R.J. Holmes, Energy Environ. Sci. (2014).

[28] P.E. Shaw, A. Ruseckas, and I.D.W. Samuel, Adv. Mater. **20**, 3516 (2008).

[29] L.A.A. Pettersson, L.S. Roman, and O. Inganäs, J. Appl. Phys. **86**, 487 (1999).

[30] See supplemental material at [URL] for HPLC data and exciton lifetime decays.

[31] N.T. Morgan, Y. Zhang, E.J. Molitor, B.M. Bell, R.J. Holmes, and E.L. Cussler, AIChE J. **60**, 1374 (2014).

[32] N.T. Morgan, Y. Zhang, M.L. Grandbois, B.M. Bell, R.J. Holmes, and E.L. Cussler, Org. Electron. **24**, 212 (2015).

[33] M. Sim, J. Shin, C. Shim, M. Kim, S.B. Jo, J. Kim, and K. Cho, J. Phys. Chem. C **118**, 760 (2014).

[34] O. V Mikhnenko, J. Lin, Y. Shu, J.E. Anthony, P.W.M. Blom, T.-Q. Nguyen, and M.A. Loi, Phys. Chem. Chem. Phys. **14**, 14196 (2012).

[35] R. Farchioni and G. Grosso, *Organic Electronic Materials: Conjugated Polymer and Low Molecular Weight Organic Solids* (Springer, Berlin, 2001).

**Figure captions:**

**Figure 1:** Absorption cross section ($\sigma_A$) and area normalized fluorescence spectrum ($F_D$) of α-NPD. The absorption cross section was calculated using the α-NPD crystal density and the extinction coefficient, extracted from ellipsometric measurements on a 40-nm-thick film deposited on silicon. The fluorescence spectrum was measured from a 40-nm-thick film deposited on glass. Inset displays the molecular structure of α-NPD.

**Figure 2:** Photoluminescence ratios versus film thickness for α-NPD films with organic purities of (a) 97.1% (b) 98.3% (c) 98.8% (d) 99.0% along with the corresponding exciton diffusion lengths ($L_D$). Solid lines represent fits based on a one-dimensional steady state exciton diffusion model at the given values of $L_D$.

**Figure 3:** Exciton diffusion length ($L_D$) of α-NPD as a function of thin film purity as measured by high performance liquid chromatography (HPLC). Solid line represents a fit of $L_D$ as a function of impurity concentration assuming exciton quenching by impurities via a Förster mechanism. The fit yields a Förster radius from α-NPD to the impurity of $R_I$ = 1.3 nm and an impurity free, maximum $L_D$ value of $L_{D,0}$ = 7.0 nm, represented by the dashed line.

**Table:**

| Organic Purity (%) | $L_D$ (nm) | $\eta_{PL}$ (%) | $\tau$ (ns) | Predicted $L_D$ (nm) |
|---|---|---|---|---|
| 97.1 ± 1.2 | 3.9 ± 0.5 | 25 ± 1 | 2.7 ± 0.1 | 4.3 ± 0.6 |
| 98.3 ± 0.8 | 4.7 ± 0.6 | 33 ± 1 | 3.1 ± 0.1 | 4.8 ± 0.7 |
| 98.8 ± 0.2 | 5.1 ± 0.6 | 34 ± 1 | 3.2 ± 0.1 | 4.9 ± 0.7 |
| 99.0 ± 0.3 | 5.3 ± 0.9 | 37 ± 1 | 3.3 ± 0.1 | 5.1 ± 0.7 |

**Table 1:** Experimentally determined values of the thin film purity, exciton diffusion length ($L_D$), photoluminescence efficiency ($\eta_{PL}$), exciton lifetime ($\tau$), and predicted $L_D$ calculated using an exciton diffusion model based on Förster theory.

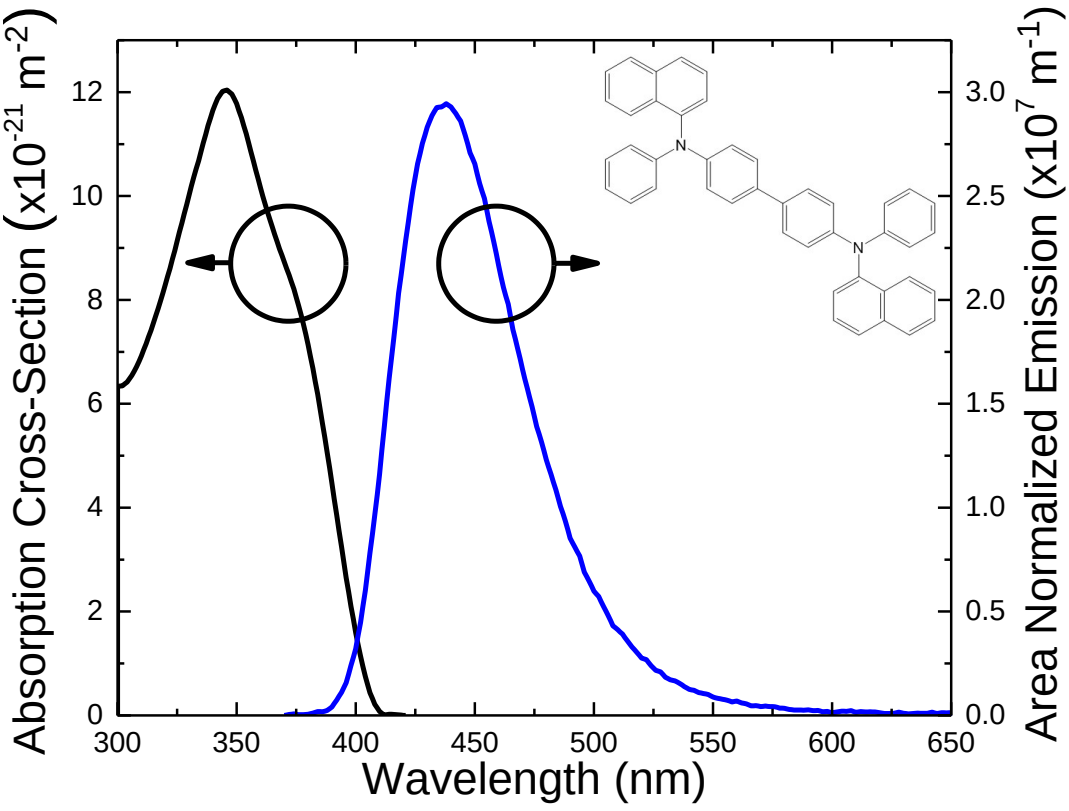


Figure 1: Curtin et al.

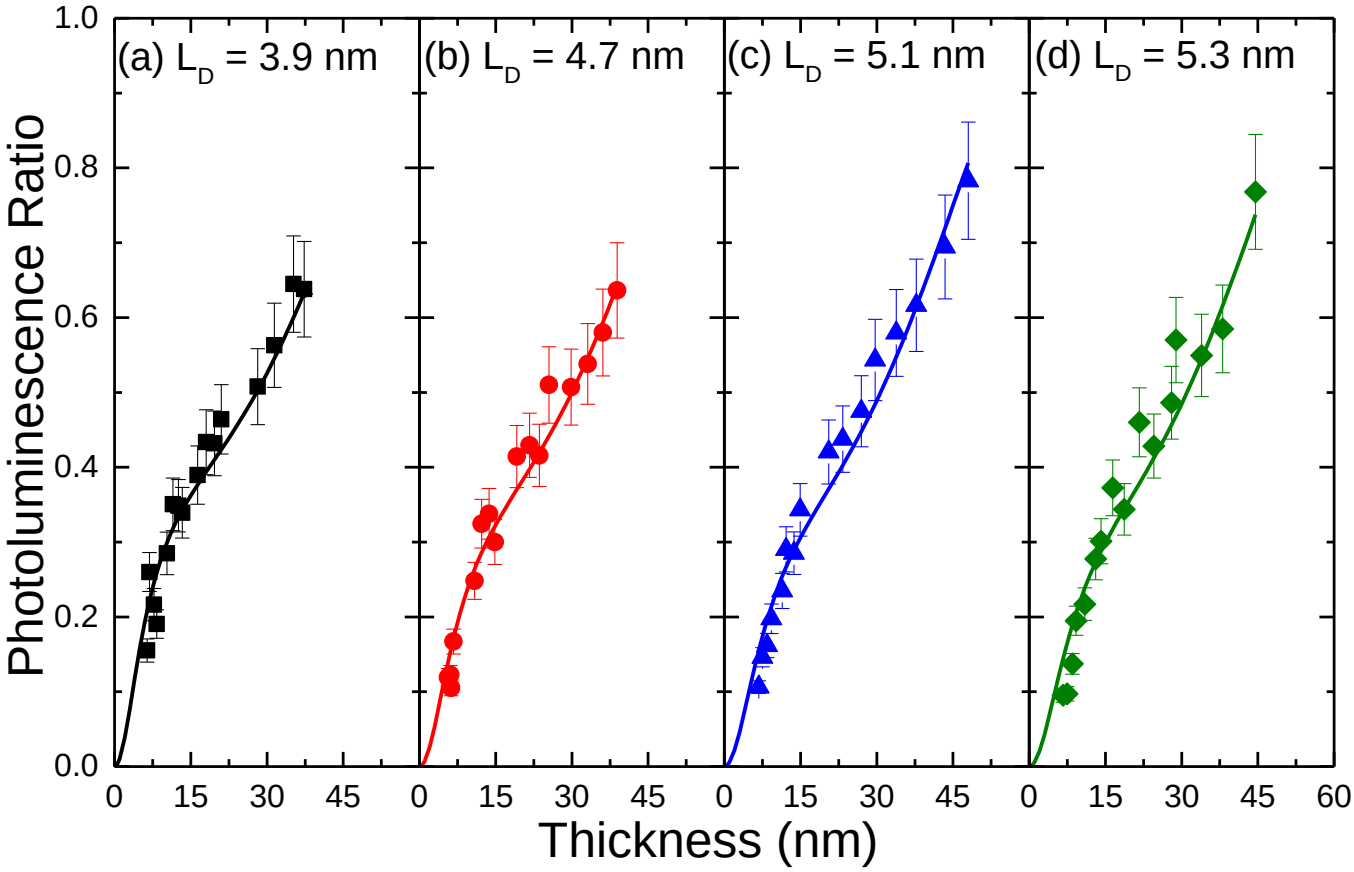


Figure 2: Curtin et al.

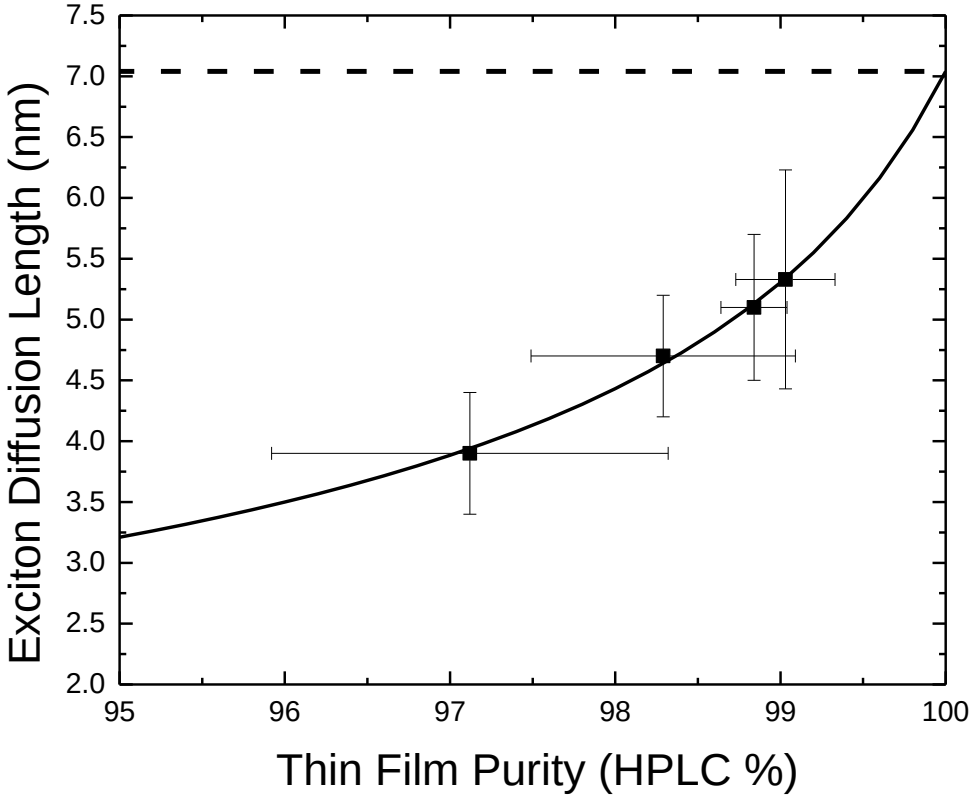


Figure 3: Curtin et al.